Multimode Fiber Raman Lasers Directly Pumped by Laser Diodes

Sergey A. Babin, *Member, IEEE*, Ekaterina A. Zlobina, and Sergey I. Kablukov

(Invited Paper)

***Abstract*—Raman fiber lasers (RFLs) are usually based on single-mode fibers core-pumped by high-power rare-earth-doped fiber lasers with single transverse mode output that leads to a rather complicated design of RFLs. One of interesting possibilities to simplify the RFL design is its direct pumping by cheap and reliable high-power multimode laser diodes (LDs). It is attractive to use standard graded-index multimode passive fibers characterized by very high quality and low cost due to their wide use in telecom. In this case, one can directly couple the multimode radiation of high-power LDs with moderate brightness into the core of multimode graded-index fiber with much higher efficiency than into the core of single-mode fiber. Using commercially available multimode LDs with operating wavelengths of 915–940 nm, it is possible to obtain high-power high-beam-quality Raman lasing in wavelength range of 950–1000 nm, which is problematic for rare-earth-doped fiber lasers. Here, we review the results obtained in this direction and report on the demonstration of all-fiber LD-pumped CW Raman laser based on the graded-index fiber. A joint action of Raman clean-up effect and mode-selection properties of special fiber Bragg gratings inscribed in the central part of fiber core, results in high-efficiency conversion of multimode (M^2∼26) pump at 915 nm into a high-quality output beam at 954 nm. Fibers with core diameter of 62.5, 85, and 100 μm are compared. With core enlargement, the conversion efficiency increases sufficiently (from 47% to 84%) at the expense of slight beam-quality parameter reduction (M^2 = 1.3–3). The generated spectrum remains to be rather narrow (<0.4 nm) at output power >60 W .**

***Index Terms*—Fiber laser, Raman laser, GRIN fiber, multimode, diode pumping, pump combiner, fiber Bragg gratings, Rayleigh scattering, single-mode output.**

I. Introduction

CW FIBER lasers have achieved in the last decade an outstanding performance in terms of output power and efficiency, beam quality and stability thus enabling their wide use in industrial applications. Most of high-power lasers utilize rare-earth (RE) doped double-clad fibers pumped by high-power multimode laser diodes into the fiber cladding. The low-quality pump radiation is guided by the multimode silica cladding and absorbed in the single-mode RE-doped core which then re-emits the high-quality laser light in the RE emission band, see [1] for a review. The most powerful Yb- doped fiber laser (YDFL) is able to deliver 10 kW diffraction-limited output beam at ∼1.07 μm [2].

In order to achieve such a high power, fiber pump combining and tandem pumping techniques have been implemented. In particular, laser diode pump sources typically pigtailed with a 105/125 μm step-index multimode fiber are connected by means of pump combiner before being launched into the RE-doped fiber [1], [3], [4]. In the tandem pumping scheme, one or several LD-pumped high-power fiber lasers pump another one [2], [4]. The tandem pumping offers several advantages for power scaling, namely, it makes possible in-band pumping so that the quantum defect heating can be low thus resulting in a reduced thermal load and reduced dimensions of the cladding since the pump with high brightness is used in the final stage, for more details see [1], [2]. It is estimated [5] that several tens kW output is feasible with the tandem pumping, but a further limitation caused by the development of mode instability comes into play [3].

Laser wavelength flexibility is another important feature of fiber lasers. They can be tuned by ∼100 nm within the gain bandwidth of RE dopants (1–1.15, 1.5–1.65 and 1.9–2.1 μm for Yb, Er and Tm/Ho, accordingly [1], [3]). Amplification via stimulated Raman scattering in passive fibers enables lasing beyond the wavelength range of RE elements, see [6] for a review. The wavelength of such Raman fiber laser can be tuned within the relatively broad Raman gain spectrum, Stokes-shifted from the pump wavelength. The Stokes shift value is defined by the vibration quanta amounting to ∼13 THz in standard telecommunication silica fibers.

Raman fiber lasers usually utilize single-mode fibers core-pumped by YDFLs or other high-power RE-doped fiber lasers with single transverse mode output beam. Such pumping scheme leads to a rather complicated design of RFLs. At the same time, Raman lasers are characterized by a small quantum defect, low background spontaneous emission and absence of photo-darkening effect, which is a problem for RE-doped fiber lasers, especially for YDFLs operating near 1 μm [1]. YDFL-pumped RFLs deliver more than 100 Watts of output power for the first [7] and higher Stokes orders generated in the nested

Manuscript received August 4, 2017; revised September 7, 2017; accepted October 12, 2017. Date of publication October 25, 2017; date of current version December 8, 2017. This work was supported by the Russian Science Foundation under Grant 14-22-00118. *(Corresponding author: Sergey A. Babin.)*

S. A. Babin is with the Institute of Automation and Electrometry, SB RAS, Novosibirsk 630090, Russia and also with the Novosibirsk State University, Novosibirsk 630090, Russia (e-mail: babin@ise.nsk.su).

E. A. Zlobina and S. I. Kablukov are with the Institute of Automation and Electrometry, SB RAS, Novosibirsk 630090, Russia (e-mail: zlobinakaterina@gmail.com; kab@iae.nsk.su).

Color versions of one or more of the figures in this paper are available online at http://ieeexplore.ieee.org.

Digital Object Identifier 10.1109/JSTQE.2017.2764072

cavities made of fiber Bragg grating (FBG) pairs reflecting all intermediate Stokes wavelengths [8]. Much simpler design (free of FBGs) utilizes broadband random distributed feedback via Rayleigh backscattering [9] providing high-efficiency cascaded generation of multiple Stokes orders in a wavelength range up to one octave, see [10], [11] and citation therein.

Power scaling of Raman fiber lasers to kW level is shown to be possible for an integrated Ytterbium-Raman fiber amplifier architecture [12]. Injecting a seed laser beam into a 1080-nm Yb-doped fiber laser in MOPA (master oscillator – power amplifier) configuration results in generation of 1.28 kW power at 1120 nm. Modification of this scheme results in 3.89 kW power even in the absence of seed [13]. Nevertheless, all these schemes are based on a high-power YDFL with some extension necessary for Raman conversion.

An interesting possibility to simplify the RFL design is its direct pumping by cheap and reliable high-power multimode LDs, similar to the LD-pumped RE-doped fiber lasers [1]–[5]. To continue the analogy, it is possible to employ cladding pumping, but this technique requires development of special double-clad passive fibers [14], [15]. In this way, Raman lasing at 1120 nm with output power of 100 W and beam quality parameter $M^2 \sim 1.6$ was demonstrated with a multimode YDFL as a pump source [14], whereas at direct diode pumping only 6 W power was obtained [15].

From technical and economical points of view, it is more attractive to use standard graded-index (GRIN) multimode fibers which currently have high quality and low cost due to their wide use in telecom. In this case, one can directly couple the multimode radiation of high-power LDs into the multimode GRIN fiber core. Low background loss of standard GRIN fibers allows one to use several kilometers long fibers thus increasing integral Raman gain. However, higher conversion efficiency is expected for shorter fibers with high-power pumping. Recent enhancement of brightness and maximum power of commercially available multimode LDs at 9xx nm are promising for development of efficient diode-pumped RFLs. Thus, using multimode LDs with operating wavelengths of 915–940 nm, it is possible to obtain high-power Raman lasing in wavelength range of 950–1000 nm, which is problematic for YDFLs. At the same time, output beam quality of the multimode RFL may be high enough due to the beam clean-up effect at Raman conversion of CW radiation in multimode GRIN fibers [16]. The beam quality is improved due to the competition between various transverse modes of the fiber. The lower-order transverse modes of a graded-index fiber tend to have good overlap with the pump modes of the fiber, while the higher-order transverse Stokes modes have a poor overlap with the pump modes. In addition, the doping density of GeO_2 has maximum in the center of the graded-index fiber core. Therefore, Raman gain coefficient, which increases with the doping density, is higher for the lowest order modes of multimode GRIN fiber. The RFL pumped by a 1.064-μm Nd:YAG laser with beam quality parameter $M^2 \sim 7$ and power ~10 W has generated Stokes radiation with beam quality parameter $M^2 = 1.66$ at 0.8 W output power [17]. Since the power of bright ($M^2 \sim 20$) laser diodes operating at ~915 and ~976 nm has reached 100 W level for a single unit

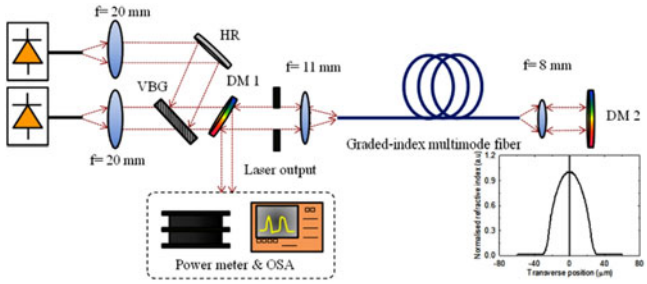

Fig. 1. Experimental setup of CW RFL based on GRIN fiber with bulk optics cavity and LD-pump coupling [15].

pigtailed by a 105-μm core fiber, the multimode RFL with direct LD pumping became feasible.

In this paper, we review recent results on the development of multimode GRIN-fiber Raman laser efficiently generating short-wavelength ($\leq$1.02 μm) high-power laser radiation with high beam quality in simple and reliable all-fiber configuration based on the multimode fiber laser technologies: direct LD pumping into the GRIN fiber core, fiber pump combining/coupling, in-core GRIN fiber cavity formed by FBGs having special 3D structure. Further developments and potential applications of this new type of lasers are also discussed.

II. Multimode Fiber Raman Lasers With Bulk Optics Cavity Pumped by 976-nm Diodes

The concept of LD-pumped RFL based on multimode GRIN fibers is actively developed in the last five years in two directions. The first one follows [17] in developing all-fiber RFL cavity by means of in-fiber FBGs operating at short-wavelength ($\leq$1 μm) with a focus on beam quality improvement [18]–[20]. In addition, possibilities of random distributed feedback based on Rayleigh scattering [21] as well as fiber coupling of pump radiation into the laser cavity [22] have been studied. The second direction focuses on power scaling capabilities studying multimode RFL with cavity based on bulk optical elements and most powerful pump LDs at ~976 nm which provide Raman lasing near 1020 nm [15], [23], [24]. Let us start the review from the second one.

Typical GRIN-fiber Raman laser configuration with bulk optics cavity is shown in Fig. 1 [15]. Beams of two high power multimode LDs operating at 975 nm are combined into a single beam at an angled narrow-band volume Bragg grating (VBG). The combined pump light is launched into a 62.5-μm core of GRIN fiber via a lens. Dichroic mirror (DM2) placed in the far end of the fiber is used to reflect the pump and Stokes light back into the fiber. It has reduced reflectivity at the second Stokes wavelength to prevent cascaded Raman generation. The left fiber end is normally cleaved and acts as a 4% output coupler. The generated output radiation is reflected by dichroic mirror (DM1) and characterized by means of power meter and optical spectrum analyzer (OSA).

Maximum output power of such RFL with a 1.5-km long GRIN fiber amounts to 19 W at slope efficiency reaching 81%. The measured quality parameter of the generated beam at 1019 nm equals to $M^2 = 5$, while it is 22 for the input pump

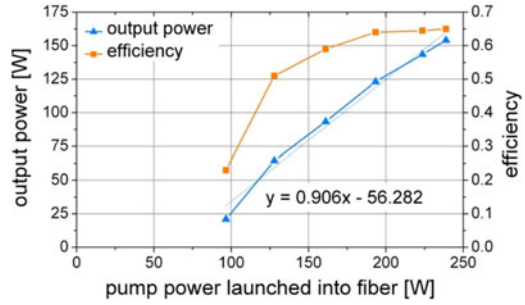

Fig. 2. Raman output power and efficiency as a function of launched pump power in a 0.2-km long GRIN-fiber Raman laser [24].

beam. Yao *et al.* [15] achieved a good agreement of the experimental and calculated power characteristics when assumed that the pump was uniformly distributed over the 1530 μm^2 effective area which is 2 times less than the core area of 3070 μm^2. Therefore, the pump intensity was more likely concentrated near the center of the core. When the GRIN fiber was replaced by 650-m special double-clad fiber, the output beam quality was improved to $M^2 = 1.9$, but the output power was reduced to 6 W because of comparatively high propagation loss in the specialty double-clad fiber.

Glick *et al.* [23] used basic configuration similar to that one shown in Fig. 1. Output Stokes power as high as $P = 85$ W at wavelength $\lambda = 1020$ nm has been obtained in a 0.5-km GRIN fiber with a high-brightness 978-nm pump LD which was operating in a quasi-CW regime of 20 ms duration and 15 Hz repetition rate. The slope efficiency of the RFL equals to 70%. The measured M^2 value of the RFL output beam varies from 2.9 to 5.6, while it changes in 12–14 interval for the input pump beam. In general, the Stokes beam quality deteriorates with increasing output power. The authors explain the reduction of the laser beam quality as follows. When the pump power increases, the Raman lasing threshold is reached in more peripheral regions of the fiber core, so those areas also begin to participate in Raman conversion and the effective Stokes beam diameter becomes larger, thus resulting in the worsening of beam quality. The brightness defined as

$$B = P/(M^2 \lambda)^2. \tag{1}$$

enhances for the Raman beam as compared to the pump one. The enhancement factor determined as the ratio of the Raman and pump brightness, takes the maximum value of 7.3 at medium power levels, the value is comparable to factor of 5.2 reported in [15].

Further power scaling was performed by adding the second 978-nm LD in the scheme and shortening the GRIN fiber length to $L = 0.2$ km [24]. The main advantage of the fiber shortening is the higher threshold for the second Stokes wave. Another advantage consists in the lower passive losses. At the same time, the reduction of fiber length resulted in the increase of laser threshold by a factor of 2.5, as compared to [23]. However, the maximum output power and slope efficiency in CW regime have also increased to 154 W and 90% correspondingly (Fig. 2). The M^2 value of the Raman output beam was measured to

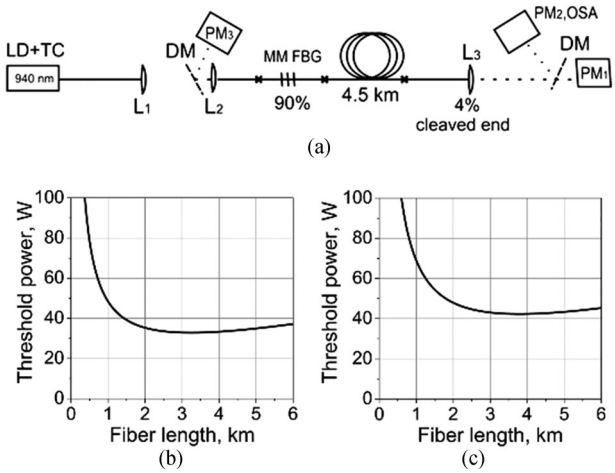

Fig. 3. (a) Experimental setup of the CW RFL with GRIN Raman gain fiber, FBG reflector (R1) and Fresnel output (R2) [18]. Calculated threshold power versus fiber length in the cavity formed by mirrors with R1 = 90% and R2 = 4% (b) or R2 = 0.7% corresponding to integral Rayleigh backscattering (c).

be between 4 to 8 at the output power increasing from 20 to 154 W while the pump beam quality before entering the fiber is $M^2 = 16 - 18$. The maximum brightness enhancement factor almost did not change (8.4) with the fiber shortening. Applying two regimes of the pump operation with different M^2 values, the authors argued that the beam quality of the Raman output weakly depends on the input pump beam quality. However, variation of M^2 value for the pump beam by 10% seems to be not enough to prove this statement. The width of the generated Stokes spectrum amounting to ~2 nm (FWHM) is determined by the Raman gain spectral profile.

Despite of the outstanding results in output power and slope efficiency obtained in [15], [23], [24], the generated wavelength of ~1020 nm is not as interesting, because a much higher power and brightness at this wavelength is available from single-mode YDFLs.

III. Multimode Fiber Raman Lasers With Fiber Cavity Pumped by 940-nm Diodes

A. FBG Cavity

In paper [18] the first CW LD-pumped RFL operating below 1 μm has been demonstrated. Pump radiation from a 938-nm LD was launched via collimating lens into a 62.5-μm core of GRIN fiber with an in-fiber cavity formed by a highly reflective multimode (MM) FBG inscribed by UV laser in the GRIN fiber core and the normally cleaved fiber end providing 4% Fresnel reflection [Fig. 3(a)]. The RFL threshold power is estimated as:

$$P_{\text{th}} = \frac{2\alpha_s L - \ln(R_1 R_2)}{2 g_R L_{\text{eff}}}, \tag{2}$$

where L_{eff} is the effective absorption length:

$$L_{\text{eff}} = \frac{1 - \exp(-\alpha_p L)}{\alpha_p} \tag{3}$$

Here $\alpha_s = 1.7$ dB/km, $\alpha_{\text{p}} = 2$ dB/km are the signal and pump attenuation coefficients, $g_{\text{R}} = 0.23$ dB (km W)$^{-1}$ is the

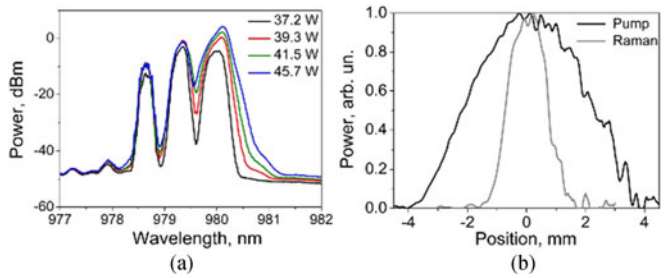

Fig. 4. (a) Output spectrum of the generated Stokes wave. (b) Output beam profile for the pump (black) and Raman (grey) laser with 4.5-km-long GRIN fiber and 90-% FBG [18].

Raman gain coefficient, R_1 and R_2 are the reflection coefficients of input and output mirrors, L is the fiber length. Following the results of calculations, the threshold power P_{th} takes minimum value in the range of cavity lengths between 2.5 and 4.5 km [Fig. 3(b)].

According to preliminary calculations, the generation threshold at wavelength 980 nm in the experiment with 4.5-km-long GRIN fiber was around 35 W. The forward Stokes power grows to 2.3 W when threshold of the 2nd Stokes wave at 1025 nm is achieved. The slope efficiency of 25% was also not high. Low value of the 2nd Stokes threshold was explained by the low-index transverse modes generation. The generated spectrum included three individual peaks [Fig. 4(a)], while the main part of the power was concentrated in the long-wavelength peak at 980 nm corresponding to the fundamental mode. The far-field profile of the output beam demonstrated a reduction of the beam divergence by three times compared to the pump beam [Fig. 4(b)].

Use of an additional mirror at the fiber end which reflected residual pump power at 938 nm back to the cavity led to the increase of the output power and slope efficiency up to 3.3 W and 35%, respectively.

B. Random DFB Cavity

On the base of this scheme, endeavors have been undertaken in order to get Raman lasing in a LD-pumped passive GRIN fiber without a conventional resonator (when Fresnel reflection is eliminated) [21]. A positive feedback in such half-open cavity can be provided by a randomly distributed Rayleigh backscattering (RS), similar to the single-mode fiber Raman lasers based on RS-based random distributed feedback (RDFB) [9]–[11]. Though the integral RS reflection coefficient in single-mode fiber is low (R∼0.1%), the scattered radiation is amplified so that the integral Raman amplification may compensate for the losses thus reaching laser threshold even in the absence of conventional cavity mirrors [9].

Experimental study of the random lasing in GRIN fiber was performed on a base of the RFL scheme with direct LD pumping [Fig. 3(a)], in which the narrow-band FBG has been replaced by a broadband mirror, and 4% Fresnel end reflection has been eliminated by cleaving the fiber end at angle >15° (against a normal one). A Rayleigh backscattering in GRIN fiber is larger than that in single-mode one. The integral RS reflection coefficient is estimated as R∼0.7%, so the RDFB lasing threshold calculated with this coefficient amounts to about 42 W [Fig. 3(c)] that has been confirmed experimentally. The generated Stokes radiation at 980 nm reaches 0.3 W or 0.5 W in the RFL configuration with or without an additional mirror reflecting back the residual pump power. High value of the threshold ∼42 W limits the available pump power above the threshold by the level of several Watts. The relative reduction of the generated beam divergence was measured to be 4.5 times as compared with that for the pump beam, i. e. it is higher than that in the case of Raman beam clean-up only [18]. Therefore, an additional influence of the RS distributed feedback and the stimulated Brillouin scattering [25] which is present near the threshold [9] make the combined clean-up effect stronger. Due to the high beam quality of the generated Stokes wave, such a laser has a very low threshold of the second-order Stokes wave generation that becomes visible in the output spectrum already at 0.5 W first Stokes power. So, to increase output power in this scheme, one should eliminate 2nd Stokes component in addition to a substantial increase of pump power.

IV. Multimode Fiber Raman Lasers With FBG Cavity Pumped by 915-nm Diodes

A. UV Inscribed FBGs

A further increase of the generated power in the GRIN fiber-based RFL with FBG cavity was achieved by optimization of the cavity length, which was obviously larger than optimal, as the transmitted pump power was relatively low (10% of the coupled pump power) in [18]. Optimization of the GRIN fiber length and utilization of the 915-nm LD pumping allowed us to increase output power and slope efficiency while decreasing the laser wavelength down to 954 nm [19].

The experimental scheme in [19] was similar to that shown in Fig. 3(a). Pump radiation from multimode LD was launched into the 62.5 μm GRIN fiber. The linear cavity of the laser was formed by high-reflection fiber Bragg grating FBG1 and normally cleaved fiber end providing weak (∼4%) Fresnel feedback, or output fiber Bragg grating FBG2 with similar reflection coefficient (∼3%). The multimode FBGs were inscribed by a high-power UV argon laser in the same multimode GRIN fiber core.

In order to increase the generated power and conversion efficiency in comparison with [18], the GRIN fiber was shortened to $L = 3.7$ and 2.5 km. Fig. 5(a) shows the residual pump (1) and generated Stokes power (2, 3) at a central wavelength of 954 nm versus input (coupled into GRIN fiber) pump power for two fiber lengths in the scheme with normally cleaved output fiber end. One can see that the experimental power threshold of ∼30 W is nearly the same for two fiber lengths, in correspondence with the calculated threshold power curve [Fig. 3(b)]. At the same time, the differential efficiency is higher for the shorter length amounting to 37% and 26% at $L = 2.5$ and 3.7 km, respectively. The total generated power reaches 4.2 W. Optimization of highly reflective grating (FBG1∗) resulted in only slight increase of the total generated power (4.7 W) and slope efficiency (41%).

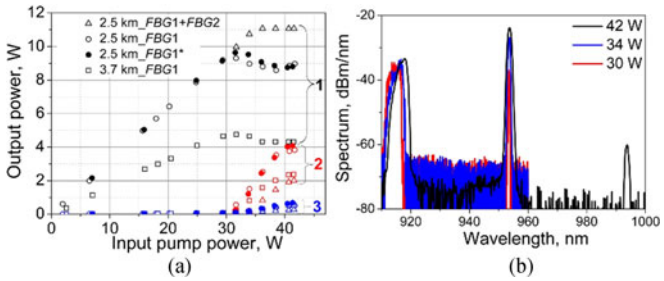

Fig. 5. (a) Residual pump power (1) and generated Stokes wave power at 954 nm in the forward (2) and backward (3) directions versus input pump power at L = 3.7 km (squares) and L = 2.5 km in the cavity formed by FBG1 and normally-cleaved fiber end (circles) or output FBG2 (triangles). Data for optimum highly reflective FBG1∗ are indicated with cross inside circle. (b) Output spectrum of RFL with 2.5-km-long GRIN-fiber at different input pump powers [19].

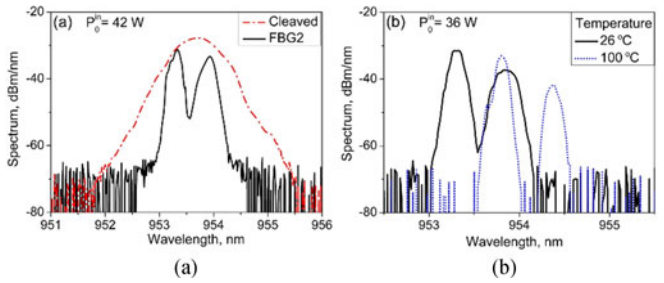

Fig. 6. Output spectra of the Stokes wave for L = 2.5 km GRIN fiber: (a) with normally-cleaved fiber end (dash-dot line) or with the output FBG2 (solid line); (b) at different temperatures of the FBG2 [19].

The second Stokes wave generation at 993 nm starts when the incident pump power exceeds 40 W [Fig. 5(b)]. Since the cascaded generation of higher Stokes orders limits the potential power for the first Stokes wave, we tried to increase the second Stokes threshold by substituting the Fresnel reflection by low reflective (3–4%) output FBG2 at 954 nm. The second Stokes was not observed, but the laser threshold was increased resulting in two-fold decrease of generation power in comparison with the normally cleaved output end.

Fig. 6(a) shows the output Stokes spectrum measured for the scheme with (solid line) and without (dash-dot line) output FBG2. The spectrum is smooth without FBG2. Its FWHM (−3 dB) linewidth of 0.7 nm is defined by the FBG1 bandwidth. With the FBG2 the spectrum has two-peak structure which is mainly defined by the FBG2. The wavelength difference $\Delta\lambda$ between two neighboring groups of the transverse modes in GRIN fiber can be estimated using equation for propagation constant and condition $\beta = \pi/\Lambda$ for reflection at FBG with period Λ [26]:

$$\Delta\lambda = \lambda^2 NA/(\pi d n_1^2), \tag{4}$$

where λ is wavelength of the fundamental mode, *NA* is numerical aperture, d is the core diameter, n_1 is the cladding refractive index. Estimated value of the wavelength difference $\Delta\lambda = 0.61$ nm is in a good agreement with the distance between two lines (∼0.62 nm) experimentally observed in the case of FBG2 [Fig. 6(a)]. Therefore those lines correspond to two neighboring groups of low-index transverse modes which are reflected by FBG2. Heating of the FBG2 to 74 degrees resulted in synchronous shifts of the two-peak structure by 0.6 nm [Fig. 6(b)]. The far-field spot size of the generated beam in the case of different output mirrors was reduced by three times in comparison with the pump beam, similar to previous results [18].

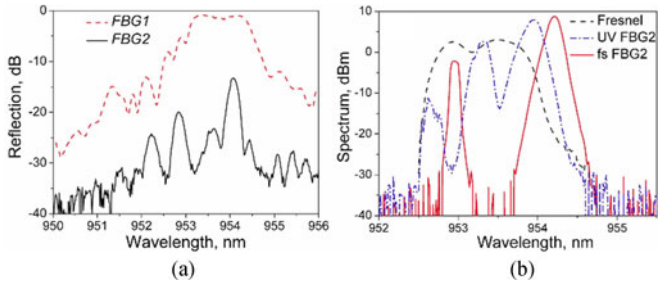

Fig. 7. (a) Reflection spectra of highly-reflective UV FBG1 (dashes) and output FS FBG2 (solid) [20]. (b) Generation spectra at 1.9 W output power for 2.5-km GRIN fiber Raman laser with different output couplers: 4% Fresnel reflection (dash), UV FBG2 (dash-dot), and FS FBG2 (solid line).

B. Fundamental Mode Selection by Femtosecond-Pulse Inscribed FBG

As the next step, a possibility of mode selection in graded-index fiber Raman laser by means of FBG was studied in [20]. To improve the selection of the fundamental mode in graded-index fiber, a special FBG was inscribed by point-to-point technique [27] in the central region of the fiber core by a femtosecond (FS) laser pulses. This FS FBG2 was spliced at the laser output instead of conventional UV FBG2 (recorded by CW UV radiation). The mode-selection properties of FS FBG2 and UV FBG2 were compared in a 2.5-km-long GRIN-fiber Raman laser (Fig. 7).

When using the highly reflective UV FBG1 and non-selective Fresnel reflection (∼4%) at the output end of the fiber, one can observe generation of a relatively homogeneous spectrum with ∼1 nm width (dashed curve in Fig. 7(b)). The reflection spectrum of UV FBG1 is relatively wide (dashed curve in Fig. 7(a)), as a result, individual resonances of transverse mode groups cannot be resolved in generation spectrum (dashed curve in Fig. 7(b)). In the case of low-reflection output UV FBG2 (which was also used in [19]), one can observe a three-peak structure with peaks spaced by ∼0.6 nm (dot-dashed curve in Fig. 7(b)) which correspond to the reflection of three individual groups of graded-index fiber modes with small transverse indices in accordance with Eq. (4). The 954-nm component corresponds to the fundamental mode, as the mode-group number increases with decreasing wavelength. The reflection spectrum is narrow for each group of modes; therefore, the generation spectra of different mode groups are well resolved. In the case of femtosecond-inscribed output grating FS FBG2, one observes a two-peak generation spectrum with a distance of ∼1.2 nm between the peaks (solid curve in Fig. 7(b)). It can be seen that the second group of modes (at a wavelength of 953.6 nm), spaced by 0.6 nm from the main one, is not involved in lasing as it is suppressed in reflection spectrum of FS FBG2 (solid curve in Fig. 7(a)).

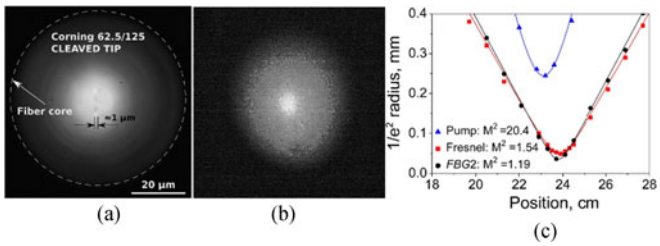

Fig. 8. (a) Microscope image of FS modification area in the core of GRIN fiber for FS FBG2. (b) Far field image of the output beam near the Raman threshold in the RFL configuration with FS FBG2. Pump beam is grey, Stokes beam is bright. (c) M2 measurement for residual pump radiation (triangles), Stokes generation in RFL with Fresnel reflection (squares) and FS FBG2 (circles) [20].

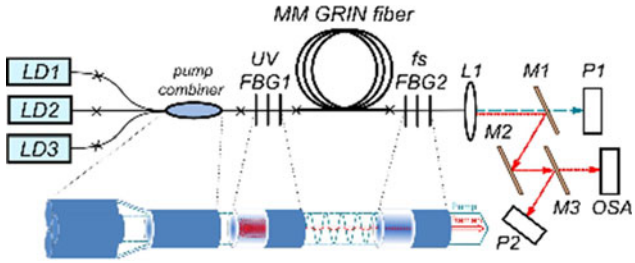

Fig. 9. Experimental setup of the all-fiber CW Raman laser with GRIN Raman gain fiber, in-fiber FBG reflectors and fiber pump combiner of three LDs [22].

Moreover, the amplitude of all the peaks related to the groups of higher order modes is relatively small. Let us also note that the generation peak at 953 nm is unstable in time and does not always manifest itself in the generation spectrum. The periodic occurrence of the additional peak at a wavelength of 953 nm (corresponding to higher order modes) was observed only in the 2.5-km-long laser. Stable single-mode lasing was obtained when the graded-index fiber length was reduced to 1.1 km.

As our measurements revealed correspondence between the FBG reflection spectra and the generation spectra (see Fig. 7(a) and (b)), let us describe in more detail the reflection spectrum of multimode FBGs in the graded-index fiber. This spectrum consists of a set of equidistant peaks with spacing according to Eq. (4). The estimation gives in our case the value of 0.61 nm, which is in good agreement with the distance between the peaks in the generation spectrum obtained with the UV FBG2. At the same time, the doubling of the distance between the peaks in case of FS FBG2 can be explained by the absence of the reflection peak for the second-group mode in its reflection spectrum [Fig. 7(a)] because of the small overlap integral for the field of this mode with the grating recorded in the central part of the fiber core.

It is known (see, e.g., [28]) that the mode-group number in a graded-index fiber can be characterized by the quantity $g = 2p + |m| - 1$, where p and m are, respectively, the radial and azimuthal mode numbers. The radial (ρ) and azimuthal (φ) field distributions for modes LP_{mp} are described by the Laguerre polynomials $L_p^{|m|}$:

$$E_{mp}(\rho, \varphi) \sim \exp(im\varphi)\exp\left(-\frac{\rho^2}{2\rho_0^2}\right) L_{p-1}^{|m|}\left(\frac{\rho^2}{\rho_0^2}\right) \frac{\rho^{|m|}}{\rho_0{}^{|m|+1}}, \tag{5}$$

where ρ_0 is the radius of the fundamental-mode field. Hence, the first two mode groups are not degenerated and contain modes LP_{01} and LP_{11}, while the third group includes two modes: LP_{02} and LP_{21}.

To estimate the overlap integral of the fiber mode field and the photomodification region in the FS FBG2, we should note that the fundamental-mode diameter $2\rho_0$ in the graded-index Corning 62.5/125 fiber can be estimated as ~9.8 μm [28], whereas the photomodification region has the form of an ellipse in the fiber cross section, with characteristic sizes of principal axes of about 1 and 10 μm as our measurements show [Fig. 8(a)]. Despite of the comparable values for the mode diameter and the photomodification region size in one of the directions, the overlap integrals are small for modes with nonzero azimuthal index m. Thus, only the modes with index $m = 0$ are maximally overlapped with the FBG recorded near the fiber core center. Therefore, only the reflection peaks corresponding to these modes (LP_{01} in the first group and LP_{02} in the third group) arise in the reflection spectrum of the FS FBG2 and, correspondingly, in the generation spectrum of the Raman laser when this grating is installed at the fiber output.

As we mentioned above, when the fiber length is shortened to 1.1 km the mode-selective properties of FS FBG2 are enough for selection of single transverse mode. As a result, nearly Gaussian beam is generated [Fig. 8(b)]. Independent characterization of the output beam in the GRIN RFL with a 1.1-km-long cavity revealed its beam quality factor M^2 is better than 1.2 at output powers up to 10 W, whereas Fresnel reflection used instead of FS FBG2 gives $M^2 \sim 1.6$ [20].

C. All-Fiber Configuration

There are so many commercial lasers based on free space structures instead of all fiberized ones. However, the all-fiber configuration has obvious advantages such as compactness, ease of operation, low cost, reliability, long-term stability and flexibility of output fiber. Thus, for practical devices it is necessary to couple the LD pump radiation via a fiber. For power scaling it is also important to combine pump radiation from several diodes. Such fiber pump combiner has been implemented in [22]. As the first step, we have compared power characteristics of the 1.1-km single-mode RFL based on 62.5 μm GRIN fiber in the schemes with bulk optics [20] and all-fiber [22] coupling of the pump radiation (Fig. 9). In the all-fiber configuration, output radiation from fiber pigtails (with numerical aperture 0.15 or 0.22) of three high-power multimode LDs operating at wavelength of 915 nm is combined by a 3 × 1 multimode fiber pump combiner. The spliced combiner has 3 input ports with multimode (MM) 105-μm core step-index fiber coupled to LDs and output port made of GRIN fiber with 100-μm core and numerical aperture 0.29. The output port is fusion spliced to the RFL cavity based on GRIN fiber with 62.5-μm core. Coupling losses for the transition from 100-μm to 62.5-μm core fiber including those at pump combiner and splices are measured to be 75%. The laser cavity was formed by the same highly-reflective (UV FBG1) and output (FS FBG2) gratings inscribed in the core of

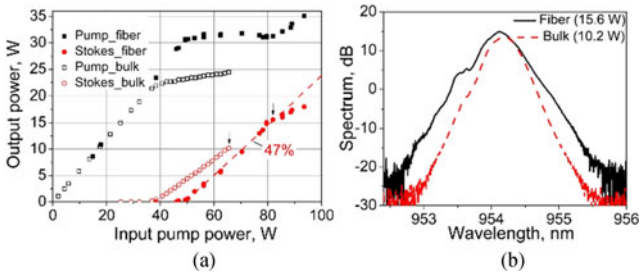

Fig. 10. (a) Power of residual pump (squares) and generated Stokes (circles) waves as a function of input pump power for the bulk-optics (empty symbols) [20] and all-fiber (filled symbols) pump coupling to the same 62.5-μm GRIN fiber with FBGs. The 2nd Stokes thresholds are shown by arrows. (b) Corresponding generation spectra at the 2nd Stokes threshold for the all-fiber and bulk-optics pump coupling configurations [22].

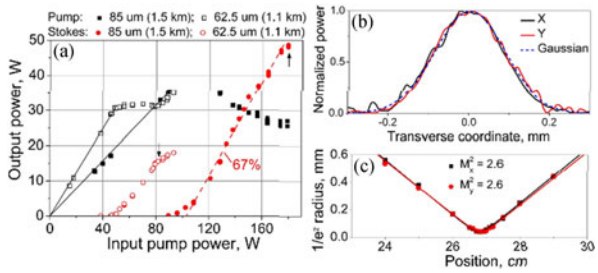

Fig. 11. (a) Output power at 954 nm (circles) and residual pump power (squares) as a function of coupled pump power for 85-μm (filled symbols) and 62.5-μm (open symbols) GRIN fiber of length 1.5 and 1.1 km, relatively (linear fit for transmitted pump in lasing-free case is shown by solid lines). Arrows show the second Stokes threshold. (b) Output beam profile for 85-μm GRIN RFL. (c) Beam radius as a function of distance from the beam waist with extracted M2 value (at 32 W output power).

the GRIN fiber (with reflection spectra shown in Fig. 7(a)). The overall schematics of all-fiber configuration are shown in Fig. 9.

The obtained power and spectra for 1.1-km GRIN RFL with different pump coupling are compared in Fig. 10. One can see that the laser generation threshold increases from ~40 W to ~50 W when changed from the bulk-optics pumping to the all-fiber one. Note that the values of transmitted pump power below the generation threshold are the same in both configurations thus confirming correctness of the comparison. The slope efficiency and the 2nd Stokes (996 nm) threshold increase from 38 to 47% and from 65 to 82 W of the launched pump power, respectively [Fig. 10(a)]. The 2nd Stokes threshold increase is reasoned by the elimination of Fresnel reflection at the input fiber facet after the modification from free-space to all-fiber pump coupling. As a result, the maximum first Stokes power at 954 nm increases from 10 W to about 16 W, whereas the generation linewidth (at −3 dB level) is left at the level of 0.4 nm [Fig. 10(b)].

The beam quality worsens only slightly from the value $M^2 \approx 1.2$ measured for the pump configuration with bulk optics [Fig. 8(c)]. The worsening manifests in the appearance of small (at −10 dB level) additional peak with wavelength of 953.5 nm corresponding to the nearest transverse mode, while for the bulk optics it is purely single-mode. At the same time, after the transition to all-fiber configuration, the RFL operation becomes much more stable.

V. Power Scaling for All-Fiber MM RFL

The combined pump power of three 915-nm LDs (each of >100 W power) is sufficient to observe Raman lasing in GRIN fiber with larger core thus enabling power scaling. For this purpose, the output port of pump combiner in the all-fiber configuration of Fig. 9 was fusion spliced to different GRIN fibers with core of 85-μm and 100-μm diameter. Herewith, the pump coupling losses are reduced to 50% and 25%, respectively.

For 85-μm GRIN fiber the measured Raman threshold amounts to ~85 W of launched pump power. Moreover, the 2nd Stokes threshold is also reached. It grows from ~135 W to ~180 W of coupled pump power at reducing fiber length from 1.95 to 1.5 km. At that, only slight increase of the first Stokes threshold (to ~90 W) is observed with the fiber shortening. As a result, maximum power at 954 nm grows from 21 to 49 W, while the residual pump power varies from 20 to 25 W only. Further shortening is not reasonable, as the maximum of available pump power is reached near the 2nd Stokes threshold. The power of 85-μm GRIN fiber Raman laser of optimal length (1.5 km) is compared with that for 1.1-km 62.5-μm GRIN RFL in Fig. 11(a). Note that 85-μm GRIN fiber FBGs have similar characteristics to 62.5-μm ones, shown in Fig. 7(a).

A comparison of the Raman lasing thresholds in the all-fiber configuration based on 85-μm and 62.5-μm GRIN fibers [Fig. 11(a)] shows that the threshold grows by almost two times in proportion with the core area increase. If the length of 85-μm and 62.5-μm fibers in the experiment would be the same, this proportion is even more accurate because the threshold power is inversely proportional to the fiber length in the region below 2 km [Fig. 3(b)]. The slope efficiency of pump-to-Stokes conversion is higher for the 85-μm GRIN fiber (67%) in spite of sufficiently stronger integral pump attenuation (compare slopes before the lasing threshold). It may be reasoned by a lower quality of the generated beam in this case. To check this, we measured the output beam profile and its radius as a function of distance along the beam waist [Fig. 11 (b) and (c)]. Fitting of this dependence gives $M^2 = 2.6$ for both axes at 32 W output power that is almost two times of the quality factor for the 62.5-μm fiber laser ($M^2 \sim 1.3$), while the beam profile appears to be close to Gaussian. The measured M^2 value is only slightly (<10%) varying with power in 10–40 W range, but sufficiently grows with the fiber lengthening ($M^2 \approx 3.1$ for 1.95 km). We have also measured parameter M^2 for the pump radiation emitted from the pump combiner output, which amounts to $M^2 \approx 26$. It is significantly higher than the value measured in 62.5-μm GRIN fiber ($M^2 \approx 21$) without pump combiner [20]. Evolution of the generated spectra with increasing power at ≈954 nm in 1.5-km fiber is shown in Fig. 12 (a).

The shape of generated spectrum is close to the hyperbolic secant with exponential wings. Its width grows as square root of the power (both for −3 dB and −10 dB levels, corresponding best-fit curves are shown in Fig. 12(b)), just like the spectrum of conventional Raman lasers based on long singlemode fibers [29], owing to an interplay of self-phase modulation and dispersion. The only sign of higher-order transverse mode impurities

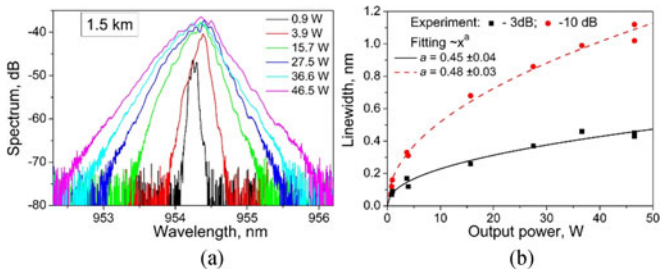

Fig. 12. (a) Generated spectrum as a function of output power in the 85-μm GRIN fiber Raman laser of 1.5 km length. (b) Corresponding linewidth values (at -3 and -10 dB levels) as a function of output power with corresponding best-fit curves.

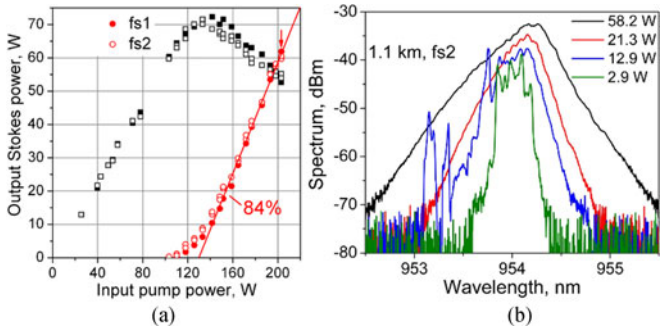

Fig. 13. (a) Output power (circles) and residual pump power (squares) as a function of coupled pump power for the 1.1-km long 100-μm GRIN fiber with different output FBGs (fs1 and fs2). The 2nd Stokes threshold is shown by arrow. (b) Corresponding output spectra at different output powers for 1.1-km-long RFL.

consists in visible asymmetry of the line shape that appears already at 4 W and doesn't change significantly with increasing power. This fact is in agreement with the weak dependence of the quality factor M^2 on the laser power. Note that the 3-dB linewidth at maximum power remains to be smaller than the distance between the neighboring groups of transverse modes: $\Delta\lambda \sim 0.45$ nm for $d = 85\ \mu$m at $\lambda = 954$ nm. We also estimate the brightness enhancement as $B_{RFL}/B_{LD} > 20$ for 85-μm GRIN RFL. It is sufficiently higher than the enhancement achieved with bulk optics in [15], [23], [24] despite of higher output power and optical efficiency in that case. So, the main factor is the better M^2 ratio provided by mode-selection properties of FBGs implemented in our case. Moreover, there is enough room for further improvement of the RFL power and efficiency thus increasing the brightness enhancement factor, for example, by means of increasing pump power with simultaneous fiber shortening and using double-pass pump configuration as in [15], [23].

At last, similar experiments have been performed with 100-μm core GRIN fiber. Lower pump coupling losses in this case provide higher maximum launched pump power (beyond 200 W from 3 diodes). At the same time, the threshold pump power has increased to ~100 W in 1.5-km fiber and only slightly changes at length variation. This provides a possibility to reduce fiber length to 1.1-km without loss in output power [Fig. 13(a)]. As a result, further increase of slope efficiency (up to 84%) and the 2nd Stokes threshold has been observed at the expense of slight reduction of beam quality. Parameter M^2 is almost independent on the generated power varying from ~2.5 to ~3.3 in output power range from 6 to 62 W. The maximum power may be sufficiently increased if one utilizes relatively high residual pump power (>50 W), similar to the schemes with bulk optics [23], [24], but for all-fiber configuration one should find an efficient solution, e.g., based on special FBGs reflecting broadband multimode pump radiation.

Note that the generated spectrum remains to be narrow, FWHM <0.4 nm [Fig. 13(b)]. However, at low powers (<13 W) it exhibits instabilities which are also observable at beam profile and M^2 measurements. The most probable reason is the mode competition, which disappears at high powers when a stable group of modes is formed with M^2 value and -3 dB spectral width almost independent of power.

The task of power scaling is also connected with the issue of choosing the optimal fiber length. It is evident that the length depends on available pump power and the cavity mirrors reflectivity. For example, for laser with normally cleaved fiber end acting as a cavity mirror the optimal length should be below 3 km which corresponds to minimal threshold pump power [Fig. 3(b)]. Increasing fiber length above 3 km results in simultaneous growth of threshold power and fiber losses. The other problem is the 2nd Stokes generation. According to [30], an efficient suppression of the 2nd Stokes component can be achieved in double-clad Raman fiber laser when the ratio of inner cladding and core diameters is less than 3. However, it becomes more difficult in multimode GRIN fibers, where mode field diameter of the fundamental mode ~10 μm is 5–10 times smaller than the core diameter. According to the experimental results presented above, the optimal fiber length enabling maximum first Stokes power at the available pump power (defined by the effect of cascaded generation) is achieved when the ratio of the threshold pump power to the maximum input pump power is around 0.5.

VI. Conclusion

Thus, the all-fiber configuration based on conventional multimode GRIN passive fiber directly pumped by fiber-coupled commercial multimode LDs at 915 nm demonstrates a possibility of generating high-power (>60 W) radiation at new wavelengths. The obtained output beam quality ($M^2 = 1.3 - 3$) is not far from that for single-mode RE-doped fiber lasers and considerably better than that for the LD-pumped Raman fiber lasers of the same power level using bulk optics for pump coupling and cavity formation [15], [23], [24]. The quality improvement in the all-fiber configuration is provided jointly by the Raman beam clean-up effect and the mode-selection properties of the narrow-band output FBG inscribed by femtosecond pulses in the central part of the GRIN fiber, which are more efficient for smaller core diameter. At the same time, the beam quality is almost independent on output power that indicates a formation of a stable group of coupled low-index modes. As a result, the shape and power broadening of generated spectrum is quite similar to those in singlemode fiber Raman lasers.

Note that this is only the first step demonstrating basic principles of the new type of CW high-power LD-pumped fiber laser.

Together with clear advantages such device has some limitations. For example, laser wavelength is limited by the available high power LDs. At the same time, it may be tuned within a relatively broad Raman gain profile. In addition, parameter M^2 worsens with increasing of the output power, in contrast to RFLs based on double-clad Raman fiber. However, RFLs with multimode LD pumping are very promising for generation of near-diffraction limited radiation at wavelengths below 1 μm in simple and robust all-fiber configuration with the prospect of power scaling to kW level. The next steps towards a better pump utilization at higher powers and a better fundamental mode selection by means of FS FBG optimization will result in further improvements in optical efficiency, output power and brightness of such source. This makes it very attractive for applications, such as efficient/bright source for pumping solid-state/fiber lasers, second harmonic generation, laser displays, bio-medical imaging.

The applications require not only efficiency and beam quality improvements, but also a broader wavelength range availability. One of opportunities is expanding this approach outside the 9xx nm wavelength range. This is possible by using commercially available CW multimode LDs at wavelength of 793 or 808 nm as a pump source for Raman laser, which has already been demonstrated in pulsed regime with the use of a highly-nonlinear fiber [31]. Power scaling of CW RFL in this case is limited by the available pump power (~50 W) of such LDs pigtailed by fibers with 105-μm core and the Rayleigh scattering losses which increase by 1.6 times when the wavelength decreases from 900 to 800 nm. Nevertheless, the demonstrated approach of all-fiber Raman laser with fiber combining and coupling of several pump LDs to GRIN fiber enables generating high-quality beam of at least tens watts power level even in the 800 nm spectral region. With the help of second harmonic generation, the RFL operating in 800–1000 nm range can be efficiently converted to visible range of 400-500 nm, which is in great demand not only for imaging/displays, but also for Raman spectroscopy and microscopy, flow cytometry, high speed printing, holography, optical data storage, laser shows, and underwater photonics [32].

Interesting fundamental challenges also appear with this type of lasers, e. g. investigation of transverse mode instability (TMI) in a graded-index passive fiber. It is known that TMI arising in step-index active fibers limits the power scaling of high power CW fiber lasers [3]. But TMI in GRIN passive fibers may behave differently from that in step-index ones, thus breaking the existing power limit caused by TMI in high power fiber lasers.

So, we believe that the first demonstrations of this new type of LD-pumped all-fiber laser with unique opportunities will inspire considerable increase of research and developments in this direction.

ACKNOWLEDGMENT

The authors acknowledge a very important input of A. A. Wolf, A. V. Dostovalov, I. N. Nemov, M. I. Skvortsov, E. I. Dontsova, V. A. Tyrtyshnyy, and D. V. Myasnikov in the performed experiments.

REFERENCES

[1] D. J. Richardson, J. Nilsson, and W. A. Clarkson, "High power fiber lasers: Current status and future perspectives," *J. Opt. Soc. Amer. B*, vol. 27, no. 11, pp. B63–B92, Nov. 2010.

[2] V. Gapontsev, V. Fomin, A. Ferin, and M. Abramov, "Diffraction limited ultra-high-power fiber lasers," in *Proc. OSA Tech. Digest Series (CD), Lasers, Sources Relat. Photon. Devices*, 2010, Paper AWA1.

[3] C. Jauregui, J. Limpert, and A. Tünnermann, "High-power fibre lasers," *Nature Photon.*, vol. 7, pp. 861–867, Oct. 2013.

[4] V. Gapontsev *et al.*, "2 kW CW ytterbium fiber laser with record diffraction-limited brightness," in *Proc. Eur. Conf. Lasers Electro Opt.*, 2005, Paper CJ-1-1-THU.

[5] J. Zhu, P. Zhou, Y. Ma, X. Xu, and Z. Liu, "Power scaling analysis of tandem-pumped Yb-doped fiber lasers and amplifiers," *Opt. Exp.*, vol. 19, no. 19, pp. 18645–18654, Sep. 2011.

[6] E. M. Dianov and A. M. Prokhorov, "Medium-power CW Raman fiber lasers," *J. Sel. Top. Quantum Electron.*, vol. 6, no. 6, pp. 1022–1028, Nov./Dec. 2000.

[7] Y. Feng, L. R. Taylor, and D. Bonaccini Calia, "150 W highly-efficient Raman fiber laser," *Opt. Exp.*, vol. 17, no. 26, pp. 23678–23683, Dec. 2009.

[8] V. R. Supradeepa, and J. W. Nicholson, "Power scaling of high-efficiency 1.5 μm cascaded Raman fiber lasers," *Opt. Lett.*, vol. 38, no. 14, pp. 2538–2541, Jul. 2013.

[9] S. K. Turitsyn *et al.*, "Random distributed feedback fibre laser," *Nature Photon.*, vol. 4, no.4, pp. 231–235, Apr. 2010.

[10] S. A. Babin, E. A. Zlobina, S. I. Kablukov, and E. V. Podivilov, "High-order random Raman lasing in a PM fiber with ultimate efficiency and narrow bandwidth," *Sci. Rep.*, vol. 6, Mar. 2016, Art. no. 22625.

[11] L. Zhang *et al.*, "Nearly-octave wavelength tuning of a continuous wave fiber laser," *Sci. Rep.* vol. 7, Feb. 2017, Art. no. 42611.

[12] L. Zhang *et al.*, "Kilowatt Ytterbium-Raman fiber laser," *Opt. Exp.*, vol. 22, no. 15, pp. 18483–18489, Jul. 2014.

[13] Q. Xiao *et al.*, "Bidirectional pumped high power Raman fiber laser," *Opt. Exp.*, vol. 24, no. 6, pp. 6758–6768, Mar. 2016.

[14] C. A. Codemard, J. Ji, J. K. Sahu, and J. Nilsson, "100 W CW cladding-pumped Raman fiber laser at 1120 nm," in *Proc. SPIE*, 2010, vol. 7508, Paper 75801N.

[15] T. Yao, A. V. Harish, J. K. Sahu, and J. Nilsson, "High-power continuous-wave directly-diode-pumped fiber Raman lasers," *Appl. Sci.*, vol. 5, no. 4, pp. 1323–1336, Nov. 2015.

[16] N. B. Terry, T. G. Alley, and T. H. Russell, "An explanation of SRS beam cleanup in graded-index fibers and the absence of SRS beam cleanup in step-index fibers," *Opt. Exp.*, vol. 15, no. 26, pp. 17509–17519, Dec. 2007.

[17] S. H. Baek and W. Roh, "Single-mode Raman fiber laser based on a multimode fiber," *Opt. Lett.*, vol. 29, no. 2, pp. 153–155, Jan. 2004.

[18] S. I. Kablukov *et al.*, "An LD-pumped Raman fiber laser operating below 1 μm," *Laser Phys. Lett.*, vol. 10, no. 8, Jun. 2013, Art. no. 085103.

[19] E. A. Zlobina, S. I. Kablukov, M. I. Skvortsov, I. N. Nemov, and S. A. Babin, "954 nm Raman fiber laser with multimode laser diode pumping," *Laser Phys. Lett.*, vol. 13, no. 3, Feb. 2016, Art. no. 035102.

[20] E. A. Zlobina, S. I. Kablukov, A. A. Wolf, A. V. Dostovalov, and S. A. Babin, "Nearly single-mode Raman lasing at 954 nm in a graded-index fiber directly pumped by a multimode laser diode," *Opt. Lett.*, vol. 42 no. 1, pp. 9–12, Jan. 2017.

[21] S. A. Babin, E. I. Dontsova, and S. I. Kablukov, "Random fiber laser directly pumped by a high-power laser diode," *Opt. Lett.*, vol. 38, no. 17, pp. 3301–3303, Sep. 2013.

[22] E. A. Zlobina *et al.*, "Generating high-quality beam in a multimode LD-pumped all-fiber Raman laser," *Opt. Exp.*, vol. 25, no.11, pp. 12581–12587, May 2017.

[23] Y. Glick *et al.*, "High power, high efficiency diode pumped Raman fiber laser," *Laser Phys. Lett.*, vol. 13, May 2016, Art. no. 065101.

[24] Y. Glick, V. Fromzel, J. Zhang, N. Ter-Gabrielyan, and M. Dubinskii, "High efficiency, 154 W CW, diode-pumped Raman fiber laser with brightness enhancement," *Appl. Opt.*, vol. 56, no. 3, pp. B97–B102, Jan. 2017.

[25] B.C. Rodgers, T. H. Russell, and W. B. Roh, "Laser beam combining and cleanup by stimulated Brillouin scattering in a multimode optical fiber," *Opt. Lett.*, vol. 24, no. 16, pp. 1124–1126, Aug. 1999.

[26] T. Mizunami, T. V. Djambova, T. Niiho, and S. Gupta, "Bragg gratings in multimode and few-mode optical fibers," *J. Lightw. Technol.*, vol. 18, no. 2, pp. 230–235, Feb. 2000.

[27] A.V. Dostovalov, A. A. Wolf, A. V. Parygin, V. E. Zyubin, and S. A. Babin, "Femtosecond point-by-point inscription of Bragg gratings by drawing a coated fiber through ferrule," *Opt. Exp.*, vol. 24, no.14, pp. 16232–16237, Jul. 2016.
[28] A. J. Mafi, "Pulse propagation in a short nonlinear graded-Index multimode optical fiber," *J. Lightw. Technol*. vol. 30, no. 17, pp. 2803–2811, Sep. 2012.
[29] S. A. Babin, D. V. Churkin, A. E. Ismagulov, S. I. Kablukov, and E. V. Podivilov, "FWM-induced turbulent spectral broadening in a long Raman fiber laser," *J. Opt. Soc. Amer. B*, vol. 24, no. 8, pp. 1729–1738, Aug. 2007.
[30] J. Ji, C. A. Codemard, J. K. Sahu, and J. Nilsson, "Design, performance, and limitations of fibers for cladding-pumped Raman lasers," *Opt. Fiber Technol.*, vol. 16, pp. 428–441, Dec. 2010.
[31] T. Yao, and J. Nilsson, "835 nm fiber Raman laser pulse pumped by a multimode laser diode at 806 nm," *J. Opt. Soc. Amer. B*, vol. 31, no. 4, pp. 882–888, Apr. 2014.
[32] J. S. Jaffe, "Underwater optical imaging: The past, the present, and the prospects," *IEEE J. Ocean. Eng.*, vol. 40, no. 3, pp. 683–700, Jul. 2015.

Sergey A. Babin was born in East Kazakhstan region (former USSR), Kazakhstan, in 1961. He received the M.Sc. degree in physics from the Novosibirsk State University, Novosibirsk, Russia, in 1983, the Ph.D. (1990) and D.Sc. (2003) degrees in physics and mathematics from the Institute of Automation and Electrometry SB RAS, Novosibirsk, Russia.

Since 2007, he has been the head of Fiber Optics Laboratory at the Institute. He and his team demonstrated random Raman fiber lasers with record parameters (efficiency, polarization extinction ratio, tuning, etc.). The problems of spectrum broadening in fiber lasers and its efficient conversion into visible range have also been solved. Fundamental limitations found and femtosecond pulses with maximum energy in an all-fiber oscillator have been demonstrated. Femtosecond technology of writing gratings through the fiber coating with unique lasing and sensing characteristics is developed. Laser and sensor systems for industrial applications (communications, biomedicine, material processing, oil and gas, infrastructure, and energetics) have been proposed and realized. His main scientific achievements include the development in collaboration with colleagues from MPE Garching of powerful laser guide star source, in 2000, and the longest fiber laser (up to 300 km) with colleagues from Aston University, in 2009. He is the corresponding member of Russian Academy of Sciences (RAS), member of OSA, IEEE Photonics Societies, and Chief Editor of Applied Photonics journal (in Russian).

Ekaterina A. Zlobina was born in Perm region, Russia, in 1985. She received the M.Sc. degree in physics from the Novosibirsk State Technical University, Novosibirsk, Russia, in 2009 and the Ph.D. degree in physics and mathematics from the Institute of Automation and Electrometry SB RAS, Novosibirsk, Russia, in 2014, where she works as a Research Fellow of Fiber Lasers Group.

Her main scientific achievements deal with the development of CW all-fiber parametric oscillator tunable in a broad range and different configurations of tunable Raman fiber lasers with random distributed feedback.

Sergey I. Kablukov was born in Krasnoyarsk region, Russia, in 1972. He received the M.Sc. degree in physics from the Novosibirsk State University, Novosibirsk, Russia, in 1994, the Ph.D. (1997) and D.Sc. (2014) degrees in physics and mathematics from the Institute of Automation and Electrometry SB RAS, Novosibirsk, Russia, where he works as a Leading Research Fellow.

Since 2015, he has been the head of Fiber Lasers Group of Fiber Optics Laboratory at the Institute. His main scientific achievements deal with research and development of broadly tunable CW fiber lasers operating in IR and visible ranges (with intra-cavity frequency doubling), as well as other nonlinear conversion and tuning techniques, such as parametric conversion, self-sweeping of fiber laser frequency, and various applications of developed devices. Recent developments also include different configurations of random fiber Raman lasers.